

## Giant Collective Fluctuations of Charged Membranes at the Lamellar-to-Vesicle Unbinding Transition. 2. Equation of State in the Absence of Salt

Bruno Demé,<sup>†</sup> Monique Dubois,<sup>‡</sup> and Thomas Zemb<sup>\*,‡</sup>

*Institut Laue-Langevin, BP 156, F-38042 Grenoble Cedex 9, France, and Service de Chimie Moléculaire, CEA Saclay, F-91191 Gif sur Yvette Cedex, France*

*Received May 15, 2001. In Final Form: September 3, 2001*

The equation of state of a charged phospholipid (dioleoylphosphatidylserine: DOPS, Na<sup>+</sup>) in the absence of added salt is given at room temperature over six decades of osmotic pressure (100 to  $2 \times 10^8$  Pa) covering the range of pressures where the different structures described previously have been observed.<sup>1</sup> It is compared to the universal expression given by the Langmuir equation and predictions for the Gouy–Chapman regime for highly charged bilayers. Below membrane separations of 10 Å, the pressure of solid supported DOPS films is higher than the prediction of the Langmuir equation. In the linear swelling regime of flat bilayers and up to the regime where giant correlated fluctuations are present (the oyster shell state), the Langmuir equation holds better than the prediction given by Attard et al.<sup>2</sup> for the Gouy–Chapman regime. Close to maximum swelling (700 Å), the pressure drops sharply. However, the universal power-law decay still holds in the unbinding regime, where the oyster shell state coexists with vesicles. The unbinding occurs as a progressive transformation of the oyster shell state into closed vesicles by a peeling mechanism of the lamellar domains.

### Introduction

The equilibrium microstructures observed upon dilution of the anionic phospholipid dioleoylphosphatidylserine (DOPS) in the absence of added salt are given in the first part of this paper.<sup>1</sup> They show the following sequence: a disordered state at low hydration, a lamellar phase with molten chains ( $L_w$ ) following a linear swelling versus  $1/\phi$ , a lamellar phase with giant correlated undulations detected by a superstructure peak (oyster shell state), and a phase of spontaneous vesicles. There is no macroscopic separation into coexisting fluids corresponding to different microstructures. The loss of smectic symmetry corresponds thus to a phase transition which is only weakly first order. The two structural features characteristic of the oyster shell state are giant undulations whose amplitude is larger than the lamellar periodicity of the stacks ( $u \gg d$ ) and correlated undulations, in phase for a whole stack of adjacent bilayers.

These two features give to freeze-etching micrographs a peculiar texture resembling that of an oyster shell, as can be seen on the micrographs.

The second part of this work is aimed at establishing the osmotic pressure decay during dilution over the whole range of concentrations and pressures where different microstructures have been observed by small-angle scattering and freeze-fracture electron microscopy (FFEM).

Even for the widely studied natural phosphatidylserines, the equation of state is not known in binary solutions. Experimental values established over a large range of equilibrium states can provide a critical test of theories for fluctuation-enhanced or fluctuation-damped long-range electrostatic interactions between bilayers.

In the case of charged phospholipids and in the absence of added salt, the relevant interactions expected are the

following: short-range steric repulsions associated with headgroup hydration, dominating when water layers are less than  $\sim 20$  Å;<sup>3</sup> the van der Waals interaction which can be derived at the level of the Lifshitz theory<sup>4,5</sup> or by taking into account the effect of counterions on screening;<sup>6</sup> and the electrostatic interaction, analytic at the level of the Langmuir equation, which uses Poisson–Boltzmann with punctual charges at the general level of charge regulation,<sup>7</sup> when no correlation effects introduced by multivalent ions are present. Counterions are considered as punctual charges in the regime where the membrane separation ( $d_w$ ) is much larger than the ion radius.

In pure water, in the case of punctual counterions only, that is, without added salt or electrolyte background due to dissociated surfactant monomers, the repulsive pressure is known as the Langmuir equation:<sup>8</sup>

$$\Pi_e(d_w) = \frac{\pi kT}{2L_b} \frac{1}{d_w^2} \quad (1)$$

where  $L_b$  is the Bjerrum length (7.2 Å in water at room temperature) and  $d_w$  is the water layer thickness. This expression does not depend on values of the elastic bending constants. The absence of screening, due to residual salt or buffers, should produce a decrease of electrostatic interactions as the square of the water layer thickness and not an exponential behavior. When a sufficiently large range of water layer thicknesses is explored, the power-law and exponential decays can be experimentally distinguished. To our knowledge, the case where only

(2) Attard, P.; Mitchell, D. J.; Ninham, B. W. *J. Chem. Phys.* **1988**, *88*, 4987–4996; *J. Chem. Phys.* **1989**, *89*, 4358–4367.

(3) Rand, R. P.; Parsegian, V. A. *Biochim. Biophys. Acta* **1989**, *988*, 351–376.

(4) Ninham, B. W.; Parsegian, V. A. *Biophys. J.* **1970**, *10*, 646–663.

(5) Parsegian, V. A.; Ninham, B. W. *Biophys. J.* **1970**, *10*, 664–674.

(6) Netz, R. R. Submitted.

(7) Mitchel, D. J.; Ninham, B. W.; Richmond, P. *J. Theor. Biol.* **1972**, *37*, 251–259.

(8) Israelachvili, J. N. *Intermolecular and surface forces*, 2nd ed.; Academic Press: London, 1991.

\* To whom correspondence should be addressed. E-mail: zemb@drecam.saclay.cea.fr.

<sup>†</sup> Institut Laue-Langevin.

<sup>‡</sup> Service de Chimie Moléculaire, CEA Saclay.

(1) Demé, B.; Dubois, M.; Gulik-Krzywicki, Th.; Zemb, Th. *Langmuir* **2001**, *17*, 997–1004.

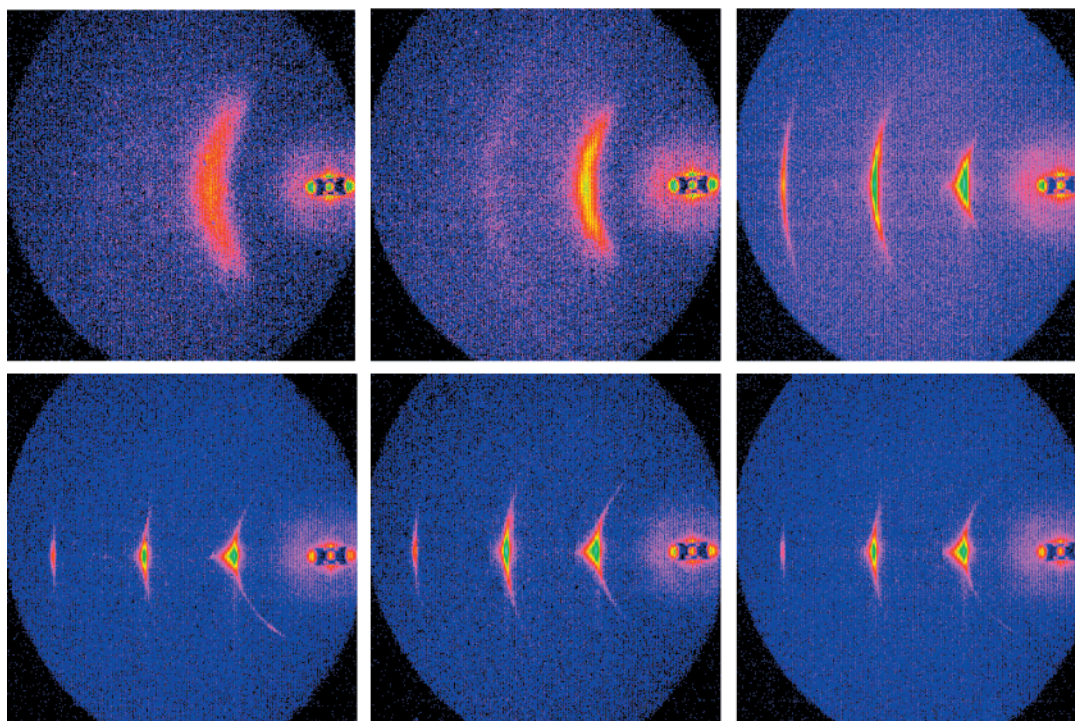


**Figure 1.** 2-D SAXS patterns obtained by grazing incidence small-angle scattering on oriented bilayers under controlled vapor pressure. From left to right, relative water vapor pressure obtained with saturated solutions of  $\text{MgCl}_2$ ,  $\text{Mg}(\text{NO}_3)_2$ ,  $\text{NaCl}$ ,  $\text{KCl}$ ,  $\text{BaCl}$ , and  $\text{K}_2\text{SO}_4$  (33%, 53%, 75%, 80%, 85%, 90%, and 95% relative humidity, respectively).

counterions are present has not been reported for charged phospholipids since the works of Cowley et al.<sup>20</sup> and Loosley-Millman et al.<sup>9</sup>

If charge regulation occurs, that is, if binding of counterions to the bilayers takes place for reasons which are independent from electrostatic terms, the net repulsion is expected to be lower than the value given by the Langmuir equation. Finally, an attractive dispersion term exists between apolar layers, complicated by the general dispersion force which occurs between a given counterion and the oil/water interface.<sup>10</sup> This attractive term, if present in DOPS, should reduce the value of the measured osmotic pressure. Detailed experiments on three different lipids have confirmed experimentally what is expected from theory: van der Waals interactions can be neglected for highly charged bilayers at any water layer thickness above 30 Å in low salt conditions.<sup>11</sup>

The general expression for dispersion forces is also known and has been compared to the repulsive terms in order to predict the maximum swelling, as well as the type of unbinding transition. Equations of state and corresponding swelling behaviors have been predicted explicitly in terms of pertinent analytic expressions by Podgornik et al.<sup>12</sup> The interplay between electrostatics, other interactions, and topology, as well as the additivity of the different interactions involved, can be tested by precise determination of the equation of state (represented by the pressure vs distance relation). This is a way of identifying the dominant repulsive interaction, as well as the first direct experimental test to our knowledge of the additivity of electrostatic and dispersion forces. The mechanism for fluctuation enhanced electrostatics between charged bilayers in the absence of salt predicts

significant deviation from the value expected according to the Langmuir equation.<sup>12</sup> Thus, we will extend the experiments as much as possible to the low-pressure (dilute) regime where the unbinding transition occurs. A first-order phase transition associated with a plateau in osmotic pressure which has already been observed in the case of cationic surfactants in the presence of residual salt<sup>13,14</sup> is expected in this range. The first equation of state of charged cationic surfactant has been established for dihexadecylammonium acetate but in the presence of added salt<sup>15</sup> (0.005–0.5 M). The pressure–distance relation was shown to be independent of the physical state of the bilayers (frozen or molten). Hence, it can be inferred that molecular protrusion forces are negligible, at least close to room temperature. We focus here on the equation of state in the absence of excess salt, using an anionic lipid. One of the aims of this study is to compare the case of DOPS to other documented cases of charged surfactant in the absence of salt. This latter was established in the case of a double-chain cationic surfactant by varying the counterion polarizability.<sup>16</sup>

## Materials and Methods

Sample preparation, small-angle neutron scattering (SANS), and freeze-fracture experiments were performed in the conditions described in the first part of the present paper. Small-angle X-ray scattering (SAXS) experiments under controlled vapor pressure were performed with an additional humidity chamber with pressure and temperature control.

The principle of establishment of the equation of state is to impose a given osmotic pressure to the sample, wait for equilibration, and characterize the microstructure. A further step

(9) Loosley-Millman, M. E.; Rand, R. P.; Parsegian, V. A. *Biophys. J.* **1982**, *40*, 221–232.

(10) Ninham, B. W.; Yaminski, V. *Langmuir* **1997**, *13*, 2097–2108.

(11) Loosley-Millman, M. E.; Rand, R. P.; Parsegian, V. A. *Biophys. J.* **1982**, *40*, 221–232.

(12) Podgornik, R.; Parsegian, V. A. *Langmuir* **1992**, *8*, 557–562.

(13) Dubois, M.; Zemb, Th.; Belloni, L.; Delville, A.; Levitz, P.; Setton, R. *J. Chem. Phys.* **1992**, *96*, 2278–2286.

(14) Zemb, Th.; Belloni, L.; Dubois, M.; Marcelja, S. *Prog. Colloid Polym. Sci.* **1992**, *89*, 33–38.

(15) Tsao, Y.; Evans, D. F.; Rand, P.; Parsegian, V. A. *Langmuir* **1993**, *9*, 233–241.

(16) Dubois, M.; Zemb, Th.; Fuller, N.; Rand, R. P.; Parsegian, V. A. *J. Chem. Phys.* **1998**, *108*, 7855–7869.



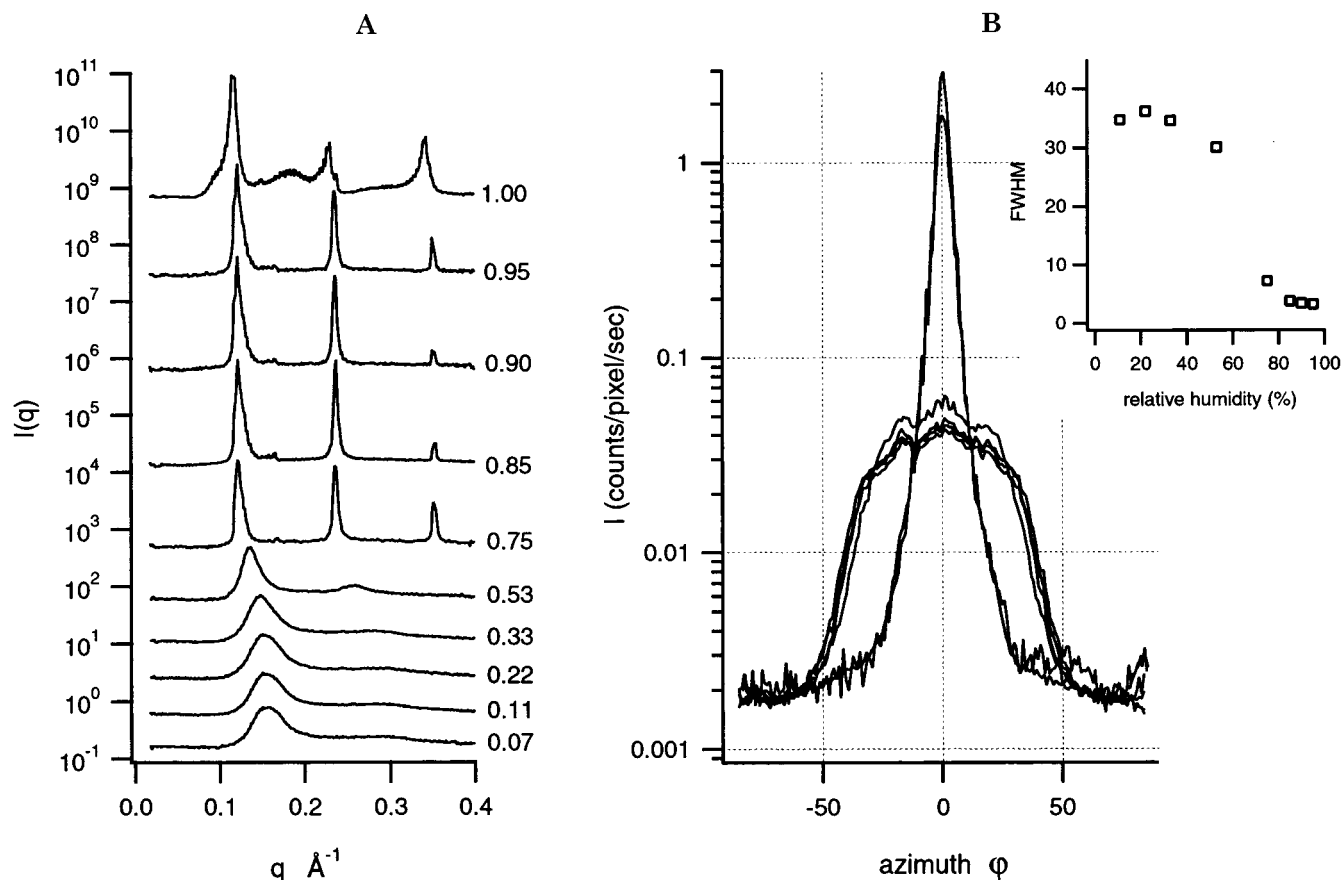


**Figure 2.** (A) Radially averaged data of a series of samples measured under controlled vapor pressure. The respective relative vapor pressures  $P/P_0$  are indicated next to the curves. The last curve corresponding to  $P/P_0 = 1$  was obtained by spreading liquid water on the film to reach saturation. It did not lead to a significant increase of swelling compared to the same sample at  $P/P_0 = 0.95$ . (B) Same series of data in azimuthal representation at the first Bragg peak position. The inset shows the sudden transition between an amorphous state with  $40^\circ$  mosaicity in the plane of the bilayers and the highly ordered  $L_\alpha$  phase with less than  $3^\circ$  mosaicity (fwhm of the azimuthal profile).

of concentration determination can be required if structural determinations do not give the direct composition of phases in coexistence. Due to the wide range (six decades) of osmotic pressures involved here, we have combined three different experimental procedures:

(1) Grazing incidence X-ray scattering on lamellar stacks supported on glass under controlled vapor pressure ( $10^7 < \Pi < 10^9$  Pa) using saturated salt solutions.<sup>17</sup>

(2) Dialysis equilibrium with dextran 110 000 solutions, imposing an osmotic pressure,<sup>18</sup> followed by SANS experiments and chemical analysis by total organic carbon determination of the sample content after several weeks of equilibration. Dialysis devices (Slide-A-Lyser cassettes from Pierce, Rockford, IL) with a membrane cutoff of 3500 were also used to allow experiments on small volumes of the order of 1 mL.

(3) Direct measurements of osmotic pressure using a membrane osmometer (AO330 osmometer, Knauer, Berlin, Germany).

Parsegian and co-workers initially described these complementary methods,<sup>18</sup> except for the commercially available membrane osmometer limited to low osmotic pressures ( $\Pi < 10^4$  Pa). Experimental procedures used here have been described in detail previously.<sup>17</sup> Using two complementary procedures, we were able to measure the swelling from the "nearly dry state" on a solid support (by equilibrating the sample with  $P_2O_5$  in the humidity chamber) to volume fractions of less than 1% in bulk.

The thickness  $d_w$  of the water layers is given by the relation  $d_w = d - 2t$ , where  $d$  is the lamellar periodicity and  $2t$  is the membrane thickness. To use this relation, it is important to

ensure that the bilayer thickness is not derived from a simple dilution plot which is valid only for flat bilayers presenting no fluctuations. In the case of DOPS, we use the density profile of the membrane determined by SAXS.<sup>1</sup> The limits of the profile give a direct measurement of the bilayer thickness with an excellent precision, independent of packing, undulations, and concentration. The high- $q$  oscillations of the membrane form factor, also observed by SANS, can be in principle fitted like the SAXS data, but the neutron scattering length density profile makes SANS less sensitive to the full membrane thickness due to the low contrast between the solvent and the layer of hydrated headgroups.

## Results

In the smectic state, the corresponding periodicities from bilayer contact to maximum swelling have been measured using SAXS and SANS. Here, the solid support is used to observe the spacing versus pressure relation in the low swelling regime corresponding to high pressures easier to obtain with vapor pressure than in bulk with concentrated polymer solutions. These experiments under controlled water vapor pressure were mainly used for pressures over  $10^5$  Pa. Osmotic stress was used for pressures below  $10^5$  Pa. Five microstructures have been encountered. Two are distinct solid supported lamellar phases: one disordered (broad quasi-Bragg peak) and poorly aligned (high mosaicity) the other one highly regular and perfectly aligned parallel to the substrate. The three other phases were observed in bulk: a swollen  $L_\alpha$  lamellar phase, the oyster shell state with correlated fluctuations,<sup>1</sup> and finally stable single or multilayer vesicles that form spontaneously.

(17) Dubois, M.; Zemb, Th. *J. Phys. IV France* **1998**, *8*, 55–65.

(18) Parsegian, V. A.; Rand, R. P.; Fuller, N. L.; Rau, D. C. In *Methods in enzymology*; Academic Press: New York, 1986; Vol. 127, pp 400–416.

**Table 1. Characteristics of the Samples Prepared by Osmotic Stress<sup>a</sup>**

log $\Pi$ (Pa)	dextran %	smectic period $d$ (Å)	undulation period $s$ (Å)	equilibrium $\phi$ (%)
1.76	0.13			0.47
1.96	0.26			0.47
1.96	0.26	700		1.54
2.5	0.94	690		2.05
2.94	2.08	587		1.91
3.02	2.34	479		1.80
3.36	3.82	474		2.38
3.52	4.73	361		3.73
3.66	5.61	319	1210	4.1
3.85	6.97	266	1050	6.31
4.27	10.82	197	630	9.25
4.68	15.74	140	280	16.77

<sup>a</sup>  $d$  and  $s$  correspond to the peaks observed by scattering. Total organic carbon analysis (TOC) gives the exact composition of the samples after equilibration.

**Disordered to Ordered Lamellar Phase ( $\Pi > 10^7$  Pa,  $d_w < 10$  Å).** Typical two-dimensional (2-D) SAXS patterns obtained with thin oriented layers under grazing incidence are shown in Figure 1 for several pressures imposed via saturated salt solutions. Broad peaks corresponding to an amorphous structure are observed for osmotic pressures exceeding  $10^8$  Pa. The radial and azimuthal averaging of the 2-D patterns in the pressure range  $2 \times 10^8 > \Pi > 10^7$  Pa are shown in Figure 2A,B. The azimuthal data were obtained from a narrow angular band centered on the position of the first quasi-Bragg peak. Both radial and azimuthal data show a peculiar behavior. Upon decreasing osmotic pressure, we observe a gradual transformation: the broad diffuse peak shows both a weak lamellar ordering (radial data) and a weak orientation (azimuthal data). Upon hydration, the broad peak transforms into a sharper peak and well-defined second and third orders appear. Narrowing of the azimuthal profile to less than  $3^\circ$  (full width at half-maximum, fwhm) indicates that the membranes orient perfectly parallel to the quartz–air interface. This corresponds to the succession of phases with frozen chains at room temperature but high concentration observed for DMPC by Janiak.<sup>19</sup>

**Rigid Lamellar Phase to Collectively Fluctuating Membranes: The Oyster Shell State ( $10^5 < \Pi < 10^2$  Pa).** Table 1 gives the values of osmotic pressure imposed by dextran 110 000 solutions in the reservoir as well as quasi-Bragg peak positions and corresponding superstructure distances,  $d$  and  $s$ , respectively. The latter is characteristic of the oyster shell state, when detected. For pressures below  $10^5$  Pa (Figure 3), the lamellar spacing is measured by SANS on bulk samples equilibrated for several weeks against dextran solutions. Using this method, only pressures of  $10^5$  Pa can be reached leading to a pressure gap between the high-pressure experiments under vapor pressure and bulk measurements. By decreasing the pressure, the lamellar spacing increases from 170 to 700 Å (see Table 1) while quasi-Bragg peaks broaden and then disappear. Several orders (up to 6) can be detected up to a spacing of 315 Å (Figure 4). In Figure 3, an additional soft correlation peak appears at low  $q$  (arrows) moving to lower  $q$  upon dilution and disappearing before the lamellar order is lost. Figure 4 focuses on a sample at  $\phi = 0.041$  and  $\Pi = 4.6 \times 10^5$  Pa where the exceptionally well ordered swollen lamellar structure is evidenced. The superstructure broad peak at low  $q$  ( $s$ ) is located at  $\sim 4d$ .

Data measured over six pressure decades are put together in Figure 5, in the log–lin representation. This

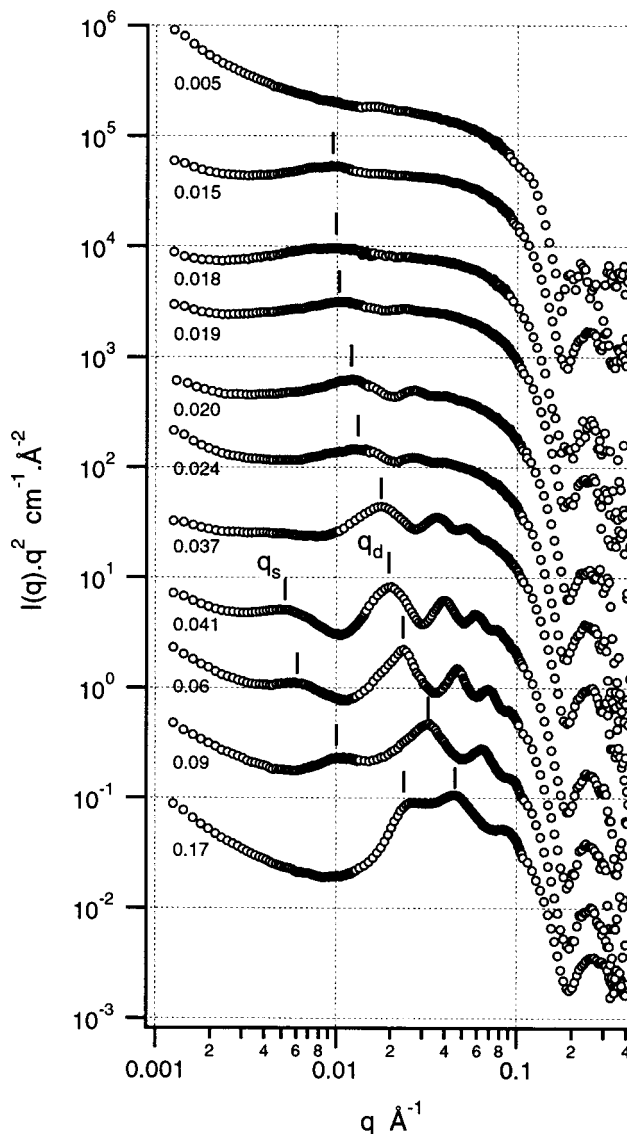


**Figure 3.** Series of SANS curves ( $I(q)q^2$  vs  $q$  plot) obtained with samples equilibrated at fixed osmotic pressures via the osmotic stress technique. From bottom to top: increasing  $d$ -spacing, with  $\phi$  varying from 0.17 to 0.005 as measured by total carbon analysis in the phospholipid compartment and after long equilibration allowing ripening of superstructures. The series evidences the gradual transformation from a stiff  $L_\alpha$  lamellar phase to the oyster shell state, with a superstructure peak ( $s$ ) corresponding to the in-plane undulation wavelength, and finally to charged vesicles ( $\Pi < 100$  Pa). The lower curve is to the scale; the others are shifted for clarity.

representation is used to detect a possible exponential decay which would result from the presence of residual salt imposing a screening length. Values obtained here with DOPS are completed in the range of  $10^5$ – $10^7$  Pa by data already available in the literature for charged membranes in the absence of added salt. These have been obtained with phosphatidylglycerol by Cowley et al.<sup>20</sup> and Loosley-Millman et al.<sup>11</sup>

## Discussion

**Osmotic Pressure versus Swelling.** Data corresponding to the different microstructures can be plotted as osmotic pressure versus smectic periodicity at fixed

(19) Janiak, M. J.; Small, D. M.; Shipley, G. G. *Biochemistry* **1976**, *15*, 4575–4580.

(20) Cowley, A. C.; Fuller, N.; Rand, R. P.; Parsegian, V. A. *Biochemistry* **1978**, *17*, 3163–3168.

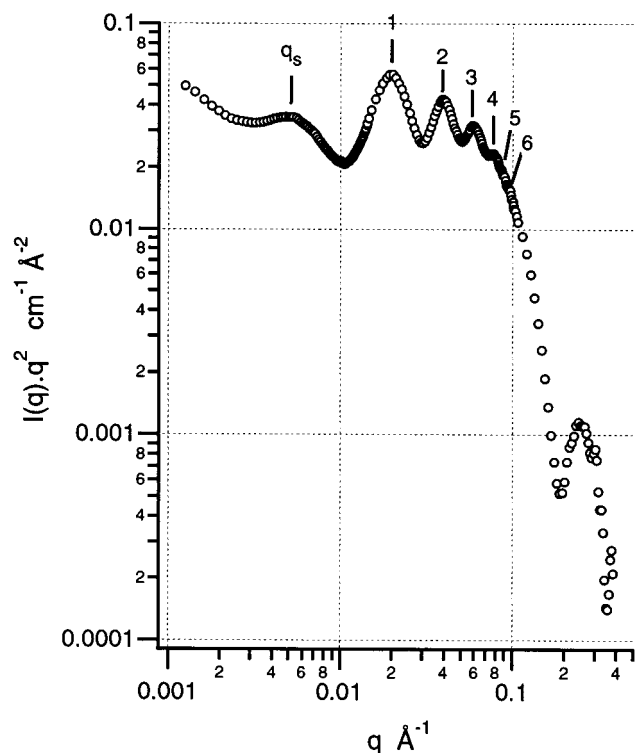


**Figure 4.** SANS curve of an equilibrated sample ( $\phi = 0.041$ ) under imposed osmotic pressure,  $\Pi = 4.6 \times 10^3$ , after several weeks of equilibration. The sample is an ordered lamellar phase ( $d = 310$  Å) showing six detectable quasi-Bragg reflections and strongly correlated fluctuations producing a superstructure peak at  $s = 1210$  Å.

temperature, that is, in the form of an equation of state. Figure 5 summarizes scattering experiments performed at imposed osmotic pressure. The range of pressures covered by the different techniques used in this work covers 6 orders of magnitude in osmotic pressure and 3 orders of magnitude in membrane separation,  $d_w$  (see also Figure 6). The absence of exponential decay in the log–lin representation shows that there is no residual salt in addition to  $\text{Na}^+$  counterions.

**Transition at High Pressure between Disordered Stacks and Regular  $L_\alpha$  Phase.** Figures 1 and 2 show a sharp transition in solid supported lamellar stacks at a vapor pressure  $P/P_0$  between 0.53 and 0.75, that is, around  $5 \times 10^7$  Pa. Hydration–dehydration sequences show that the transition is completely reversible. This transition cannot only be related to chain melting, since long-range order appears together with hydration. In this range of membrane distances, the pressure observed is larger than what is predicted by the Langmuir equation except for  $d_w < 10$  Å. The average counterion concentration is in the range of 2–20 M, and steric effects in the Stern layer are dominant. No obvious exponential decay from hydration forces is observed in this regime. Surprisingly, the maximum swelling obtained by equilibration with vapor pressure is much lower than what is observed in bulk. The situation here resembles the vapor paradox, which has been recently solved,<sup>21</sup> but the difference here is of 1 order of magnitude in spacing, and spreading of liquid water on the sample does not increase significantly the swelling (1 Å). Furthermore, one should keep in mind that solid supports are not adequate to measure large

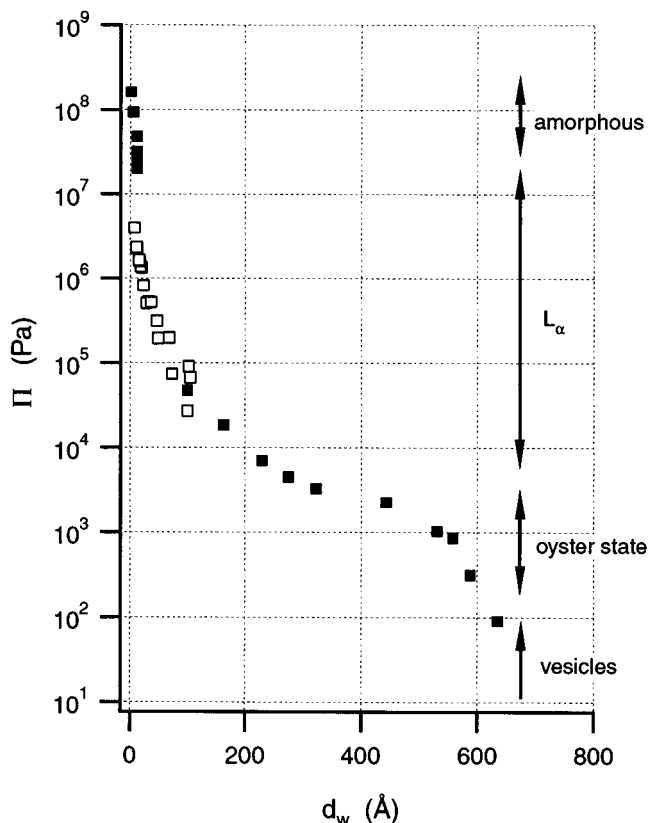


**Figure 5.** Osmotic pressure  $\Pi$  vs distance curve of DOPS (■). The points at short distances are from the SAXS experiments under controlled vapor pressure ( $d_w < 10$  Å). Large distances were obtained by osmotic stress at room temperature. Intermediate points (□) are data taken in the case of the anionic phospholipid phosphatidylglycerol by Cowley et al. (ref 20) and Loosley-Millmann et al. (ref 11) in the absence of added salt as well. The log–lin representation used in this plot evidences the absence of exponential decay of the pressure. This demonstrates the absence of background electrolyte producing a “Debye screening length” due to residual charged species other than free counterions between bilayers.

periodicities of strongly fluctuating lamellar systems because of damping effects in the vicinity of the interface.<sup>22</sup>

**Swelling in the Lamellar Regime.** When the water layer thickness exceeds 100 Å, the pressure measured is in good agreement with the prediction given by the Langmuir equation. Below 10 Å, the important deviation from the purely electrostatic contribution may be due to steric effects, to hydration forces, or to the fact that the sample is solid supported. None of these effects is considered here. Swelling turns from sterically to electrostatically dominated (Stern layer dominant). As already shown in part 1 by SAXS and SANS, the position of the first minimum of the membrane form factor gives direct evidence that the bilayer thickness is independent of concentration in the range of concentrations studied here in bulk. Thus, values of the periodicity  $d$  can be directly converted into separation distances  $d_w$ . This is different from the case of shorter chain lipids, where bilayer thickness increases when osmotic pressure decreases.<sup>16</sup> In Figure 5, we have put together our experimental data obtained with DOPS with data obtained by Cowley et al.<sup>20</sup> and Loosley-Millman et al.<sup>11</sup> with another anionic phospholipid, phosphatidylglycerol, also studied in the absence of added salt.

(21) Katsaras, J. *Biophys. J.* **1998**, *75*, 2157–2162.

(22) Salamat, G.; de Vries, R.; Kaler, E. W.; Satija, S.; Sung, L. P. *Langmuir* **2000**, *16*, 102–107.



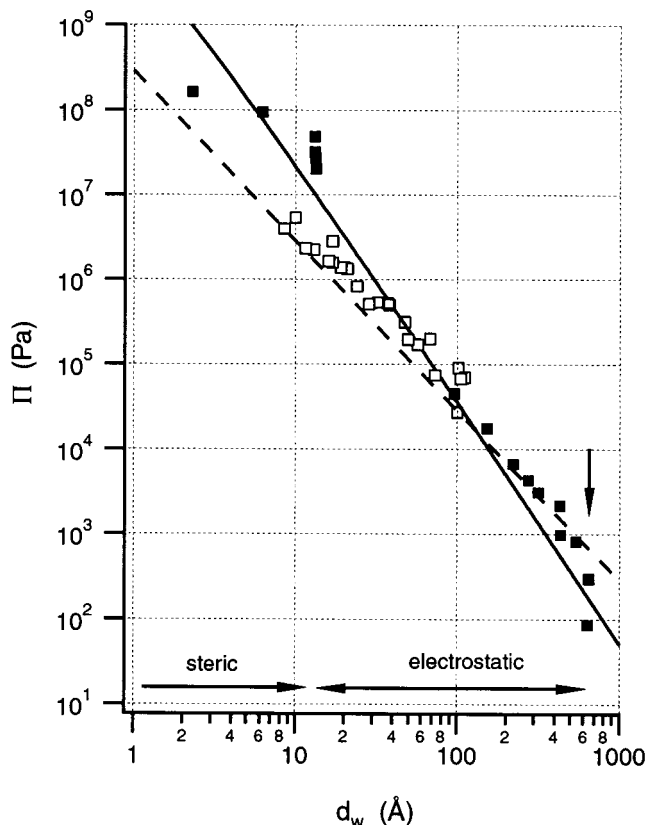


**Figure 6.** Log–log representation of the pressure  $\Pi$  vs distance curve (same data as Figure 5). The dashed line is calculated according to the Langmuir equation (eq 1), and the solid line is the relation proposed by Attard et al. (ref 2) (eq 2). This representation evidences the dominant electrostatic repulsion in the case of counterions only. At pressures exceeding  $10^7$  Pa, steric terms come into play and the pressure is higher than pure electrostatics. In the regime where the electrostatic repulsion is the dominant interaction, the Langmuir equation holds. At  $10^3$  Pa (arrow), the pressure drops sharply toward complete unbinding. The same symbols as in Figure 5 are used.

The evident nonlinearity demonstrates self-consistently that no salt (background or impurity) induces a measurable Debye screening length. Also, no exponential enhancement by uncorrelated fluctuations<sup>23</sup> is observed. In the past, screening by residual charged species has limited investigations of charged lipid bilayers in the absence of salt, as reported in the case of the synthetic cationic surfactant DDABr.<sup>24</sup>

In the present case, electrostatic interactions are dominant and long-range order is shown by the sharpness of quasi-Bragg peaks. However, undulations lead to a progressive broadening until the structure factor disappears. While lowering the imposed osmotic pressures, an asymptotic behavior toward a swelling of 700 Å is shown in Figure 6.

In previous studies, the swelling of DMPS has been described in the presence of variable concentrations of monovalent salt by Hauser and co-workers.<sup>25,26</sup> They noticed that the maximum swelling, that is, the distance where the osmotic pressure is expected to vanish, is dependent on the nature of the added salt, but in the absence of salt the swelling is limited to 105 Å. Again, in

the case of DMPS but in the same domain of concentration and ionic strength, Cevc et al.<sup>27</sup> and Copeland and Andersen<sup>28</sup> have measured and explained the effect of dilution and pH on the lamellar phase with molten chains ( $L_\alpha$ ). Chain melting is shifted from 35 to 50 °C when the net charge per head of DOPS is zero due to neutralization of the negative groups. In our case (DOPS, no added salt), the observed maximum swelling is much larger ( $\times 6$ ) than in these previous studies (Figure 3).

The power-law behavior is shown in Figure 6 where data of Figure 5 are shown in log–log representation. The Langmuir equation, predicting a  $d_w^{-2}$  decay in the so-called high charge limit, is the universal relation which considers the electrostatic repulsion between two charged planes facing each other.<sup>8</sup> The equation of state established experimentally for DOPS is in good agreement with this relation for  $100 \text{ \AA} < d_w < 500 \text{ \AA}$  (Figure 6). This behavior results from the unscreened electrostatic interaction due to the absence of residual salt in the case of a charged lipid with only sodium counterions.

However, we keep in mind that sodium ions are strongly coupled to the bilayers. The Gouy–Chapman length  $\lambda$  is the distance required to gain/lose  $1 kT$  in free energy for one given counterion. Numerically, the Gouy–Chapman length is given by  $\lambda = \sigma / (2\pi L_b)$ , where  $L_b$  is the Bjerrum length (7.2 Å in water). The area per molecule  $\sigma = 62 \text{ \AA}^2$  is given by the molecular volume of DOPS<sup>3</sup> (1350 Å<sup>3</sup>) and the known thickness of the membrane 44 Å (see part 1). The Gouy–Chapman length is then 1.4 Å for DOPS. Most counterions are thus condensed in the first nanometer, that is, a thickness largely below the water layer thickness. The distribution of remaining counterions presents no gradient between bilayers. The midplane theorem<sup>8</sup> identifies the osmotic pressure with the activity of counterions at  $d_w/2$ . We are here in a typical range of millimoles. In that regime,  $d_w \gg \lambda$  and a prediction by Attard et al. is available:<sup>2</sup>

$$\Pi \approx \frac{k_b T}{d_w^3} \left[ 2 + \frac{\pi}{2} \ln \left( \frac{d_w}{\lambda} \right) \right] \quad (2)$$

We compare this prediction to our experimental data in Figure 6. At the swelling cutoff which appears as a deviation from the Langmuir equation, data are closer to the Gouy–Chapman regime given by eq 2, but the slope of the experimental decay is significantly different from this prediction.

In the dilute regime limit, this prediction has been recalculated by Lukatsky and Safran<sup>29</sup> with slightly different numerical constants. It is markedly different from the power-law decay ( $d_w^{-3/2}$ ) calculated as the perfect-gas limit.<sup>30</sup> This would give a different slope too, incompatible with our experimental results.

de Vries,<sup>31</sup> using a theory developed by Odijk,<sup>32</sup> considers the case of large undulations occurring at high charge in the condition  $\kappa d > 10$ . In the case of DOPS, we have  $\kappa^{-1} \sim 100 \text{ nm}$ ,  $d_{\text{max}} = 70 \text{ nm}$ . We are in a regime where de Vries predicts no fluctuation enhancing of the electrostatic term and no damping either. Considering the pressure–distance relation, the asymptotic swelling appears as a

(27) Cevc, G.; Watts, A.; Marsh, D. *Biochemistry* **1981**, *20*, 4955–4965.

(28) Copeland, B. R.; Andersen, H. C. *Biochemistry* **1982**, *21*, 2811–2820.

(29) Lukatsky, D. B.; Safran, S. A. *Phys. Rev. E* **1999**, *60*, 5848–5857.

(30) Pincus, P. A.; Safran, S. A. *Europhys. Lett.* **1998**, *42*, 103–108.

(31) de Vries, R. *J. Phys. II France* **1994**, *4*, 1541–1555.

(32) Odijk, T. *Langmuir* **1992**, *8*, 1690–1691.

(23) de Vries, R. *Phys. Rev. E* **1997**, *56*, 1879–1886.

(24) Dubois, M.; Zemb, Th. *Langmuir* **1991**, *7*, 1352–1360.

(25) Hauser, H.; Shipley, G. G. *Biochemistry* **1983**, *22*, 2171–2178.

(26) Hauser, H.; Paltauf, F.; Shipley, G. G. *Biochemistry* **1982**, *21*, 1061–1067.

cutoff in Figure 6. This cutoff corresponds to the progressive transformation of the oyster shell state into closed vesicles.

Since the Langmuir equation gives a good evaluation for the universal high charge–large condensation regime (Gouy–Chapman length  $\lambda = 0.14$  nm), we can expect a similar behavior with double-chain surfactants with two net charges per headgroup. Indeed, phase diagrams and maximum swelling of dialkyl phosphates<sup>33,34</sup> are remarkably similar to those of lipids with a single net charge. Equation 2 with the condition  $d_w \gg \lambda$  also holds. In the case of divalent headgroups,  $\lambda$  is divided by  $2^3$  with respect to the single net charge case.<sup>35</sup>

Salditt and co-workers<sup>36</sup> have shown that the effective bilayer stiffness and hence the Caillé model are incompatible with Bragg peak shapes observed for dilute lamellar phases in the case of DMPC when interaction is strong enough so that undulations between adjacent layers are correlated. This is the case in the range of pressure where the oyster shell state is present. The Caillé model is not adapted to describe fluctuations in charged bilayers, because undulations are large compared to periodicity and bilayers are stiff. In the Gouy–Chapman regime, full expressions have been given by Fogden,<sup>37,41</sup> but the simplest analytical result has been given by Andelman:<sup>38</sup>  $k_c/kT \approx 0.06 d_w/L_b$ , that is, of the order of  $6 kT$  in the oyster shell state when spacing is ca. 100 times the Bjerrum length.

Figure 4 shows a typical scattering curve obtained after a long equilibration time (weeks) for an imposed osmotic pressure of  $4.6 \times 10^3$  Pa (imposed by 5.61 wt % dextran in dialysis reservoir). Chemical analysis of the lipid phase shows that the lipid content is 0.041. For a single-phase lamellar sample at that volume fraction and for a membrane thickness of  $44 \text{ \AA}$ ,<sup>1</sup> the corresponding periodicity should be  $1070 \text{ \AA}$ . However, the measured periodicity is only  $315 \text{ \AA}$ . This indicates that excess water is used to form more dilute nonlamellar domains (e.g., vesicles). The sample is therefore composed of approximately 70% vesicles, in equilibrium with 30% undulating lamellar phase producing the sharp reflections that can be seen. For lower volume fractions, the progressive unbinding of the lamellar structure occurs. The oyster shell state corresponds to fluctuations which dampen the quasi-Bragg peaks. From this oyster shell state, spontaneous vesicles peel off progressively upon decreasing osmotic pressures, as observed on electron micrographs.

**Spontaneous Unilamellar Vesicle Formation upon Dilution ( $\Pi < 300$  Pa).** Spontaneous vesicles in nonbirefringent samples are observed for volume fractions of the order of 0.01 (Figure 4). While going from the lamellar state to closed vesicles, there is a loss of symmetry. Therefore, a first-order transition is expected. However, we could never separate macroscopically two coexisting fluids, one birefringent and one isotropic. Furthermore, there is no pressure plateau in the pressure–distance curve. This indicates that there is no equilibrium between two distinct phases in coexistence but a continuous

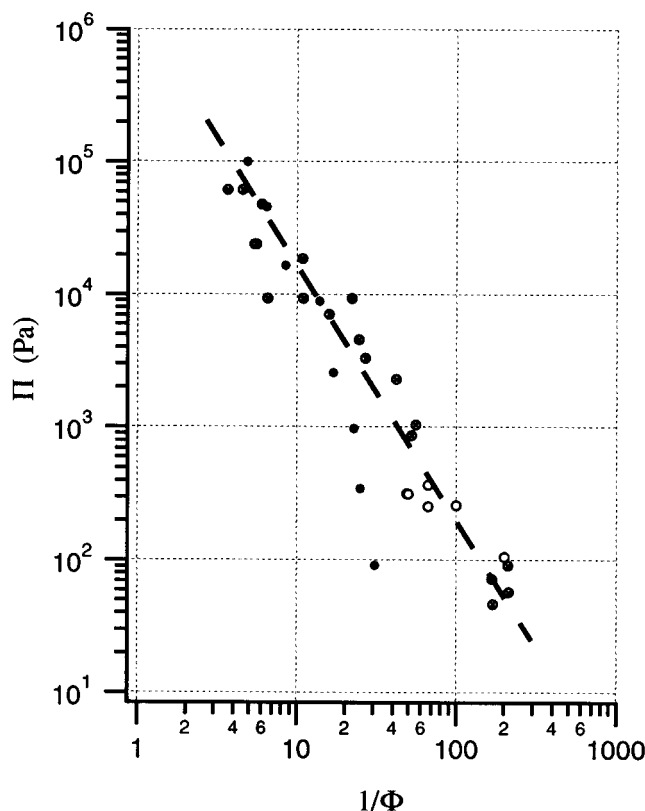


**Figure 7.** Osmotic pressure  $\Pi$  vs  $1/\phi$  at  $25^\circ\text{C}$ . The pressure results from two different techniques: osmotic stress with dextran solutions ( $\otimes$ ) and direct pressure determination of the samples with a membrane osmometer ( $\circ$ ). The dashed line is a guide to the eye representing a  $\phi^{-2}$  power law decay. The DOPS data are compared to those for DDAB ( $\bullet$ ) (ref 13). In this case, a residual  $\text{Na}^+$  concentration of  $5 \times 10^{-4}$  M led to a partial screening of the electrostatic interaction which turns from the power-law decay (unscreened case of DOPS) to the exponential behavior.

topological transformation between objects of different topology. Thus, complete unbinding results from a progressive transformation from the oyster shell state into vesicles.

A refined evaluation of the total electrostatic free energy involves repulsion between stacks of bilayers explicitly or implicitly the bending energy as a deformation of the double layer and hence the bending constants associated with a given bilayer/counterion combination.<sup>39</sup> Theoretical evaluations of bending constants ( $\kappa$  and  $k_b$  associated with mean and Gaussian curvature, respectively) are known in the absence of salt<sup>40,41</sup> with the remarkable feature that the Gaussian energy term highly favors closed objects dominated by the energy of counterions in the high dilution limit. Ninham has proposed another driving force of spontaneous vesiculation: asymmetry of inside and outside average counterion concentrations.<sup>42</sup> To ensure electroneutrality, the average inside concentration exceeds 0.1 M. The corresponding ionic strength and screening of lateral interactions between charged headgroups reduce the area per head on the inside layer by a few percent, thus inducing a spontaneous curvature toward the inside,

(33) Streefland, L.; Yuan, F.; Rand, P.; Hoekstra, D.; Engberts, J. B. *Langmuir* **1992**, *8*, 1715–1717.

(34) Fonteijn, T. A.; Hoekstra, D.; Engberts, J. B. *Langmuir* **1992**, *8*, 2437–2447.

(35) Netz, R. R.; Moreira, A. G. *Europhys. Lett.* **2000**, *52*, 705–711; *Eur. Phys. J. D* **2001**, *13*, 61–66.

(36) Salditt, T.; Munster, C.; Lu, J.; Vogel, M.; Fenzl, W.; Souvorov, A. *Phys. Rev. E* **1999**, *60*, 7285–7289. Munster, C.; Salditt, T.; Vogel, M.; Lu, J.; Siebrecht, R.; Peisl, J. *Europhys. Lett.* **1999**, *46*, 486–492.

(37) Fogden, A.; Daicic, J.; Kidane, A. *J. Phys. II* **1997**, *7*, 229–248.

(38) Andelman, D. In *Structure and dynamics of membranes*; Lipowsky R., Sackmann, E., Eds.; Elsevier: Amsterdam, 1995; pp 603–640.

(39) Fogden, A.; Ninham, B. W. *Adv. Colloid Interface Sci.* **1999**, *83*, 85–110.

(40) Fogden, A.; Daicic, J. *Colloids Surf., A* **1997**, *129/130*, 157–165.

(41) Fogden, A.; Daicic, J.; Mitchell, D. J.; Ninham, B. W. *Physica A* **1996**, *234*, 167–188.

(42) Radlinska, E. Z.; Zemb, Th.; Dalbiez, J. P.; Ninham, B. W. *Langmuir* **1993**, *9*, 2844–2850.

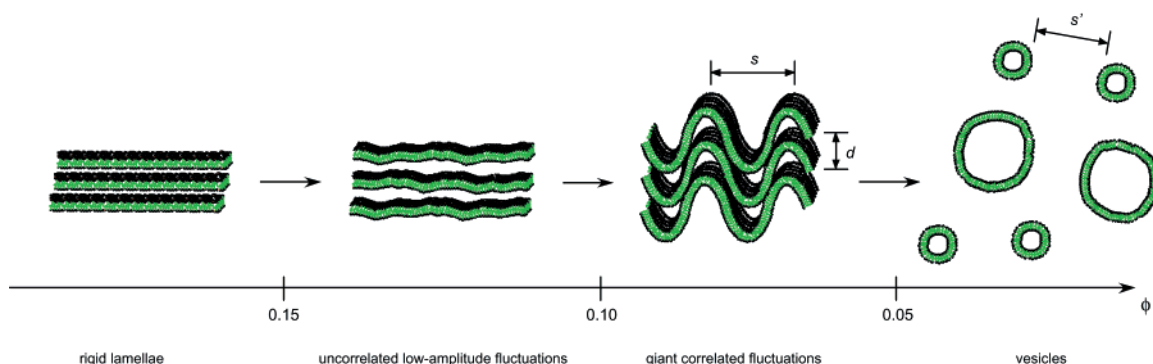


**Figure 8.** Sketch of DOPS bulk microstructures in four identified states: the rigid lamellar phase, the lamellar phase with low-amplitude uncorrelated fluctuations, the oyster shell state with the giant collective fluctuations, and vesicles nucleated from the oyster shell state. The unbinding transition corresponds to the progressive transformation of the oyster shell state in vesicles of approximately the same size as the in-plane undulation length in the oyster shell state.  $d$  corresponds to the smectic periodicity.  $s$  is the in-plane wavelength of the giant undulations appearing at moderate osmotic pressure ( $10^2$ – $10^4$  Pa). When the sample is essentially composed of vesicles, the weak and broad correlation peak observed on SANS curves corresponds to mean distance  $s'$  between bilayers of adjacent vesicles resulting from the strong unscreened electrostatic repulsion.

a mechanism driving spontaneous large unilamellar vesiculation upon dilution.

In the vesicle regime, a broad interaction peak is visible (Figure 8, part 1). The maximum of the scattering corresponds to distances in the range  $d_{cp} = 600$ – $900$  Å, a typical spacing for close-packed unilamellar vesicles:

$$d_{cp} = \frac{3}{8} \frac{2t}{\phi} \quad (3)$$

Vesicles spontaneously formed by DOPS are of the same size as the spontaneous small unilamellar vesicles discovered by Talmon et al. in cationic double-chain surfactants in the absence of salt.<sup>43</sup>

This distance  $d_{cp}$  is of the order of the in-plane superstructure peak apparent on Figure 4. When only vesicles are present, these highly charged objects produce a broad correlation peak in the same  $q$ -range.

**Equation of State Expressed vs  $1/\phi$ .** If now we consider the volume fraction  $\phi$  as a thermodynamic quantity, as plotted in Figure 7, the picture changes completely. Instead of an asymptotic pressure behavior (Figure 6), a  $\phi^{-2}$  power law is obtained in the full range of pressures/distances studied in the dilute regime. Each sample, after equilibration, is analyzed chemically in order to obtain the exact lipid concentration.

Is the van der Waals attraction sufficient to induce a partial unbinding? There is a possibility for partial unbinding, as calculated by Netz.<sup>44</sup> As can be seen in Figure 7, the power law predicted by Netz in the case of a short-range potential is also valid for unscreened electrostatics in the regime where no peak is detected by scattering. In this representation, there is no cutoff followed by a plateau which would be the signature of a partial unbinding.

The unbinding transition of charged bilayers appears as a weak second-order transition with a continuous decrease of the osmotic pressure with concentration. This corresponds to continuous formation of vesicles nucleated in the oyster shell state. The size of these vesicles is linked to the typical distances in the oyster shell state,  $s$  corresponding to the in-plane undulation wavelength and also the out-of-plane large fluctuation  $\xi_{\perp}$ . These two quantities are approximately equal and correspond to the typical size (1000 Å).

During the lamellar-to-vesicle unbinding transition, the electrostatic interaction is enhanced by fluctuations, as predicted by Podgornik and qualitatively expected from renormalization arguments. Comparing the experimental results with the predictions for unbinding by Podgornik and Parsegian,<sup>45</sup> we notice that progressive unbinding was predicted in the case of fluctuation-enhanced electrostatic interaction. However, in the case of DOPS, collective undulations between adjacent bilayers avoid the occurrence of fluctuation-enhanced repulsions.

To our knowledge, continuous formation of unilamellar closed vesicles from a “reservoir” made of stacks of correlated undulations proposed here is a new structural underlying mechanism for unbinding. We are here in the intermediate regime predicted by Podgornik and Parsegian: enhancement by fluctuations of the electrostatic interaction is compensated by the large-scale softening of the membrane. Comparing unbinding in the case of DDABr to that of DOPS with  $\text{Na}^+$  as counterion, we notice that the enhancement of electrostatic interaction by fluctuations is less pronounced because of the dispersion force between the polarizable ion ( $\text{Br}^-$ ) and the oil–water interface.<sup>10</sup>

The same data corresponding to the equation of state, expressed in pressure versus the most probable distance between bilayers (the peak in scattering) or pressure versus volume fraction (inversely proportional to molar volume), appear qualitatively different. Considering the position of the scattering peak as field variable, the electrostatic interaction is screened by fluctuations. Using volume fractions as a thermodynamic variable, the electrostatic interaction appears as enhanced by fluctuations. This experimental result established in the counterion only case represents a challenge for explicit predictive theories including both statistical thermodynamics of counterions and topology of the unbinding, such as the work of de Vries<sup>23</sup> who pointed out that bending constants may be integrated over all in-plane fluctuation lengths in order to understand the observed compressibility, expected to be exponential.

We are now in the situation where we can explain the origin of the complex scattering patterns appearing after long ripening of the structure during osmotic equilibrium. At high concentration ( $\phi > 0.10$ ), strong peaks indexed 1,2,3... arise from smectic periodicity ( $d$ ). In the oyster shell state, a weak peak ( $s$ ) appears in the region  $q < 10^{-2}$

(43) Talmon, Y.; Evans, D. F.; Ninham, B. W. *Science* **1983**, *221*, 1047–1048.

(44) Netz, R. R. *Phys. Rev. E* **1995**, *51*, 2286–2294.

(45) Podgornik, R.; Parsegian, V. A. *Langmuir* **1992**, *8*, 557–572.



$\text{\AA}^{-1}$ . The peak observed in the three most dilute samples in Figure 3 arises from vesicle–vesicle interaction, that is, from the most probable distance between bilayers in a microstructure which does not contain any remaining lamellar crystallite (samples are not birefringent and appear as composed by vesicles only using FFEM). This distance is shown as  $d$  on Figure 8.  $d$  is the two-dimensional equivalent of the correlation hole observed for polyelectrolytes.

Lowering the osmotic pressure between the oyster shell state and unilamellar vesicles, there is a possible intermediate state with closed multilayer vesicles, which has been evidenced in the presence of weaker electrostatic repulsion.<sup>46</sup> This possible intermediate microstructure has not been identified in the case of binary DOPS/water solutions. On the contrary, it has been observed that the diameter of the vesicles produced is of the order of the in-plane undulation wavelength in the oyster shell state, suggesting a peeling mechanism from the oyster shell state to the spontaneous unilamellar vesicles. The open question is whether it is general that the unbinding occurs as a progressive formation of unilamellar vesicles from the oyster shell state or if the first vesicles formed have an average number of layers of the order of 5–10. This value comes from the ratio of length to in-plane correlation in the undulation instability. In the present determination of the equation of state, we have not encountered this intermediary structure.

---

(46) Dubois, M.; Zemb, Th. *Curr. Opin. Colloid Interface Sci.* **2000**, *5*, 27–37.

## Conclusion

We have established the equation of state at room temperature of a charged lipid in pure water, dioleoyl-phosphatidylserine with its sodium counterion only (DOPS,  $\text{Na}^+$ ). We have shown that the order–disorder transition associated with the lamellar phase unbinding into vesicles is preceded by the presence of a state of strongly coupled undulating membranes, with giant collective fluctuations of adjacent membranes, producing a texture analogous to that of an oyster shell as observed by freeze-fracture electron microscopy. In the large swelling limit, the pressure decays as a power law. Unbinding occurs via progressive transformation of the undulating oyster shell state into closed vesicles.<sup>43</sup> The experimental equation of state in the absence of salt is established on the full sequence of structures.

The experimental results described here make it possible for theoreticians to think quantitatively about the dramatic effect of fluctuations in a charged lamellar system. The next step will be to rationalize the unexpected inversion of the Hofmeister series, that is, the fact that the most polarizable counterions induce the largest swelling. This has been experimentally demonstrated by Loosley-Millman et al.<sup>11</sup> but not yet explained by any theory to our knowledge.

**Acknowledgment.** The authors are grateful to L. Belloni and R. Netz for helpful discussions.

LA0107244